

Optimization of three-dimensional disassembly line with green and economic objectives using I-ACO

Yanggang Teng^{1*}, Jinjie Chen¹, Ting Chen^{1,2}, Guilin Ge¹

¹ University of Shanghai for Science and Technology, No. 516, Jungong Road, Yangpu, Shanghai

² Changzhou University, No.21, Gehu Middle Road, Wujin, Changzhou

Corresponding Author Email: hawk_teng@163.com

https://doi.org/10.18280/ama_c.730304

ABSTRACT

Received: 25 July 2018

Accepted: 28 August 2018

Keywords:

R-AOG, three-dimension disassembly line, dynamic table update, green and economic disassembly, I-ACO

Although the problem of disassembly line balance has been studied in depth, there are fewer starting points from green, economy and position as the basis for path planning. This paper considers the disassembly path from the three perspective. For green perspective, even if the product doesn't have the economic value, the toxic solid and liquid must be excluded; For economic, the re-utilize value of the disassembled object is fewer, the complete disassembly will abandon; Furthermore, the three-dimensional information is difficult to obtain. In this paper, the reducer drawn by Solidworks to obtain the position and mass, and then the improved R-AOG (Rectangle-AND/OR Graph) used to represent the directional relationship of large-scale component disassembly. And use R-AOG de-sign Allowed, Lastly, compare I-ACO with other ACO to prove the efficiency and quality, and applies it to the reducer disassembly planning to obtain the optimal disassembly path, these experimental results help company to better plan the disassembly line, reduce the maintenance threshold of the reducer, and also beneficial to build automated disassembly lines.

1. INTRODUCTION

In 2017, China's scrapped vehicles amounted to 8.58 million, which is expected to reach more than 9 million in 2018. And only 1.74 million vehicles were recovered, with a recovery rate of only 20.3%. Compared with major developed country, the recycling efficiency of China's used motor vehicles still at a very lower level [1]. As a necessary component for automobiles, gear reducer contains large number of high value parts and recyclable resource, such as shafts, bearings, gears and iron, high-quality steel, which have greater reuse value. In the life cycle of vehicles, the reducer also needs to be disassembled for maintenance. Therefore, planning a reasonable disassembly line is significance to construct green manufacturing system and promote the life cycle management of reducer.

Disassembly line balance problem (DLBP, Disassembly Line Balancing Problem) research is great significance to protect the environment, save resource and reduce maintenance costs. In recent years, scholars have used waste mechanical and electrical products (Waste Mechanical and Electrical Products, WMEP), such as printers, dishwashers, washing machines, radios, mobile phones, computers, etc., Lots of research have been done on the disassembly sequence of WMEP. In literature [2], takes the printer disassembly as example, uses the mixed fish swarm algorithm, and simulates the annealing sequence to improve the algorithm's ability to jump out of local optimum; The literature [3] take the dishwasher as example, based on ISM (Interpretative Structural Modeling method), parts reach matrix and directed graph, calculate the structural depth of the part as the basis for the disassembly sequence; In literature [4] takes the dishwasher as an example, proposes partial destructive disassembly, the

undirected graph replaces part constraint and derives the disassembly sequence plan of the component. The literature [5] uses radio as example to construct Precedence Diagram. In the case of determining workstation (with Fixed Number Workstations), for the tasks of 22, 34, 47, 60, and 73, the maximum benefit of disassembly is obtained; In [6], mobile phone and computer disassembly are taken as examples to construct four objective functions f_1 , f_2 , f_3 , and f_4 , to obtain minimum number workstations, fluency index, remove the number of hazardous parts, obtain high value parts, use HDABC (Hybrid Discrete Artificial Bee Colony) solves FDLBP (Fuzzy Disassembly Line Balancing Problem) and compares ABC, DABC, HDABC three algorithms to solve the SI (Smoothness Index) of 25, 47 parts fuzzy disassembly, verifying the effectiveness of HDABC; The literature [7] uses BS (Beam Search) algorithm to treat the disassembly as assembly reverse, and define the physical and functional constraints assembly and disassembly. Select user-defined products, radio, hand lamp, compares Random Search for NS, CPU and other parameters. The result proves the high efficiency of BS; In [8], the MCDM (Multi-criterion Decision Making) method is used to establish a fuzzy trigonometric function to comprehensively consider economic, environmental and disassembly efficiency; and the effectiveness of the algorithm is verified by standard inspection procedures; The literature [9] considers various uncertainty of disassembly. In uncertain factors, the opportunistic constraint algorithm model and the genetic neural network algorithm were selected to calculate disassembly route, however, only 17 parts of the intermediate shaft of the reducer were selected for disassembly; The literature [10] also employed the idea of disassembling intermediate shaft in [9]. SCDS (Selective Cooperative

Disassembly Sequence Planning) is proposed to consider different influencing factors of the disassembly process, at the same time, OHDT (Operation-dependent Hierarchical) is used to analyze the disassembly sequence and level, establishes the priority matrix P , then use the specific matrix $E=[e_{jk}]$ represent part relationship in OHDT, and finally uses the cooperation matrix $C=[c_{jk}]$ to describe and solve the parallel of the selective disassembly problem, but there is no actual disassembly data used and the approximate tasks runs simultaneously.

In summary, the current research mainly has the following problems:

(1) Part disassembly is limited to the plane, and the components are assumed to be two dimensional directed graphs during modeling and calculation, regardless of the actual spatial distribution of the parts;

(2) Most of the disassembly time of the parts adopts random fuzzy time or assumes that the disassembly time of each part is same, which may be quite different from the actual; (iii). Only considers the time disassembly cost of the parts, and does not consider other costs of disassembly;

(3) Most of the WMEP are scrapped, not every product and every part has the need for complete disassembly;

(4) For the disassembly of multiple identical parts, only consider it as a disassembly task. There will be a large deviation from the actual situation. In order to improve these issues to be optimized, this paper proposes an improved Ant Colony Optimization (I-ACO) based on green and economic criteria, and test the algorithm using deeply researched TSP/DVRP problem. Lastly, applied to the disassembly line planning of all parts in the reducer, and the data such as the three-dimensional disassembly path map was obtained. These experimental results help company to better plan the disassembly line, reduce the maintenance threshold of the reducer, and also beneficial to build automated disassembly lines.

2. RESEARCH PROBLEM AND METHOD

The existing literatures on the DLBP, focuses on fixed workstations or assign workstations with disassembly time, disassembly tool change numbers and disassembly waiting times etc., as statistical evaluation indicators. This paper considers that the disassembly line (DL, Disassembly Line) is different from the assembly line (AL, Assembly Line): 1. It is not necessary to complete all the disassembled objects; 2. The disassembly line should consider the cost of disassembly in addition to the unexpected time; 3. The smooth time as the basis for the distribution of workstations is quite different from the actual. Therefore, the main research of this paper are as follows:

(1) To facilitate the description of the directional relationship of large scales component disassembly, use the improved R-AOG instead of the AOG directed graph;

(2) Analyze the strength of the main components such as shafts, bearings, gears, etc. and use this as economic disassembly criterion;

(3) Use Solidworks for gearbox designing and measurement, get the barycenter $P_n(x_n, y_n, z_n)$ and other parameters of each part;

(4) Improve ACO, add dynamic candidate table Allowedk, use 2-Opt for path optimization, and compared with existing literature to prove the effectiveness of the I-ACO;

(5) Two-dimensional TSP/DVRP has been studied in depth, and transform TSP/DVRP to three-dimensional disassembly path optimization.

Due to the disassembly line planning with many factors affected. To ensure the smooth progress of the research, the following assumptions are made:

(1) A task only disassembles one part, steps P39, P40, P41, P44, P45, P46, disassemble 3 parts, bolt, nut and washer. To simplify the calculation, the quality of nut and washer is included in the bolt;

(2) The route taken by the ant represents the disassembly sequence and does not represent the actual disassembly distance;

(3) The unit disassembly cost of the part $Cost_i$ reference [11] may differ from actual disassembly costs;

(4) After the I-ACO accesses all the disassembled parts, it is not necessary to return the starting point;

(5) The disassembled parts consider three values, reuse, remanufacture, and waste utilization;

(6) The barycenter of the part $P_n(x_n, y_n, z_n)$ only represents the spatial position of the disassembled component in the reducer;

(7) When removing the front and rear pins, the pins can be pulled out by wrench, it is considered to be disassembled using the same tool;

(8) The route taken by the ants multiplied quality of the parts, which is considered to be the disassembly energy consumption, as a reference for measuring the disassembly cost;

(9) When removing the covers, due to the frictional adhesion with the box, it may be necessary to use the previous disassembly tool, but in the calculation, the tool conversion number is not included;

(10) Before the algorithm runs, disassembly tools have prepared: T1Wrench, TScrewdriver, T2Wrench, Tplier, TClamp, THammer;

(11) Since the key and the shaft are tightly connected, during the actual disassembly process may need auxiliary. This paper assumes flat pliers use can achieve smooth disassembly;

(12) This article is a fixed workstation disassembly, and the workstation has no idle time.

2.1 Mathematical model

At present, the research on the disassembly line objective function focuses on minimum workstation, the minimum idle time of workstation, workstation disassembly smooth index, minimum disassembly direction changes, and acquisition of high-value parts [12-19]. The research target of this paper is optimization the three-dimensional disassembly line with green and economic objectives. Therefore, the number of disassembly direction changes in the literature is corrected to the number of disassembly tool changes, remove hazardous parts, the shortest disassembly distance and minimum energy consumption index proposed in this paper are taken as the disassembly objective function F , and the three-dimensional coordinate position, disassembly order, mass, etc. are taken as independent variable. The mathematical formulas are described as follows:

$$f_1 = \sum_{i=1}^n Tool_{ij}, Tool_{ij} = \begin{cases} 1, Tool_i \neq Tool_j; \\ 0, Tool_i = Tool_j; \end{cases} \quad (1)$$

$$f_2 = \sum_{i=1}^n M_{Pi} \times D_{ij}; \quad (2)$$

$$f_3 = \sum_{i=1}^n Task_i \times H_{Pi}, H_{Pi} = \begin{cases} 1, Part_i \text{ is hazardous;} \\ 0, Part_i \text{ is't hazardous;} \end{cases} \quad (3)$$

$$\min F = (\sum_{k=1}^3 \varphi_k \times f_k), (k \in 1,2,3) \quad (4)$$

s.t.

$$D_{ij} = D_{ji}, \forall i, j = 1, \dots, n; \quad (5)$$

$$D_{ij} = \sqrt{(x_i - x_j)^2 + (y_i - y_j)^2 + (z_i - z_j)^2} \quad (i \neq j) \quad (6)$$

$$\sum_{i,j \in p} P_{ij} \leq |Part| - 1, 2 \leq |Part| \leq n - 2 \quad (7)$$

$$Part \subset \{1, \dots, n\}$$

$$\sum_{i=1}^n P_{ij} = 1, \quad i = 1, \dots, n; \quad (8)$$

$$\sum_{j=1}^n P_{ij} = 1, \quad j = 1, \dots, n; \quad (9)$$

$$P_{ij} = \begin{cases} 1, i \text{ can be disassembled before } j; \\ 0, i \text{ can't be disassembled before } j. \end{cases} \quad (10)$$

$$T_{ij} = \begin{cases} 0, \text{ if } T_i = T_j; \\ 1, \quad T_i \neq T_j; \end{cases} \quad (11)$$

Equation 6 is the Euclidean distance between the two parts, |Part| indicates the number of parts in the part set, Equation 7-10 ensures that each part passes once, and Equation 11 indicates the function value when the removal tool is changed.

2.2 R-AOG Graph

For AOG (AND/OR Graph) [20-21], though it is clearly showing all possible disassembly and directional relationship of a small-scale product. The current literature on AOG research focuses on about 20 parts, beyond this range, it is difficult to express the disassembly constraint relationship of components with arrows, dotted and solid arcs. In order to simplify the calculation, some literatures replace multiple identical parts with one node, and equivalent multiple parts into one part in the calculation. This will affect the disassembly sequence solution, which is quite different from the actual disassembly. The total number of disassembled parts of WMEP selected in this paper is 84, and the number is large. For example, the random disassembly of 10 bolts of P39-P48 will produce ten thousand of disassembly sequences, and if the traditional AOG is used, the directional disassembly relationship of the parts will not be clearly described. Based on this, in order to facilitate the constraint relationship of components, this paper proposes an improved AOG, R-AOG to indicate the directional relationship of large-scale component disassembly.

As shown in Figure. 1. The order of component removal in the dotted rectangle is not constrained and can be arranged arbitrarily. Some possible routes are as follows:

39-41-43-45-42-46-47-48-44-40;40-44-48-46-47-45-42-43-41-39;46-42-48-45-41-46-47-43-44-40;

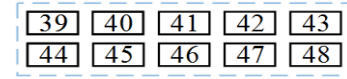


Figure 1. OR Graph

The solid rectangle indicates that the components in the frame must be removed in the order of arrangement. As shown in Figure. 3, the removal order must be: 66-67-68-69-70 and 71-72-73-74-75;

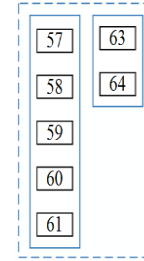


Figure 2. AND/OR Graph

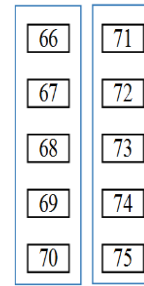


Figure 3. AND Graph

The large dotted rectangle indicates that the order of removal in the frame except the solid rectangle can't be changed, there is no disassembly constraint relationship, as shown in Figure. 2, the possible disassembly route is: 57-58-59-60-61-63-64 or 63-64-57-58-59-60-61.

2.3 Green and economic disassembly guidelines

There are little existing literatures combine the dismantling economy with green production. The dismantling research on WMEP mostly ignores the residual harmful substances in products and the time to eliminate these hazards, etc., ignoring the significance of green economy dismantling on corporate compliance and environmental protection. There are five major criteria for green production [22]: hazardous materials, energy, carbon emissions, toxic waste, solid waste, which from an environmental perspective, reduces carbon emissions, and the early removal of toxic solid waste to prevent pollution, protect public health and comply with relevant regulations is important. From economic view, all tasks must be completed on the assembly line to achieve production goals, but in disassembly line, consider the economics of disassembly, not every disassembly object must be disassembled or completely disassembled. If important parts are severely damaged and there is no repair value, the complete disassembly should be abandoned. According to the idea of green and economic disassembly, remanufactured, reused, and waste-utilized parts have enormous environmental and economic value:

(1) Compared to manufacturing new parts, remanufacturing can achieve 60% energy savings, 70% of raw materials,

reducing costs by about 50%, and reducing emissions by more than 80%;

(2) Compared with manufactured new parts, the disassembly cost of part P_{40} is $COST_{P_{40}}=0.088$, which reduces the cost by 69% compared with the market price of about 0.28, and saves raw materials and reduces the use of various resources;

(3) Waste utilization and literary creation. In China, most tourist attractions, shopping malls, and creative culture markets use WMEP make character models, such as scrapped car parts reducers, wheels, etc. by welding to made a Transformers. In addition, compared with the use of materials such as plastics, not only save manufacturing costs, but also reduces waste of resources, and has a longer service life, and has low maintenance costs.

Due to the force of the main components such as gears, shafts and bearings, are all the input shaft torque T_l or T_l 's transformed force. And the parts that can be clearly observed from the peephole are only gears. Therefore, the state of the gear is used to measure the maintenance situation of the reducer. According to the basis of maintenance status, when designing the ant walking route, the cover plate is preferential-ly removed and increased by 15 seconds to determine if or not to completely disassemble. The strength and life check formulas for gear, shaft, and bearing are as follows:

$$\sigma_{H|gear} = 5Z_E \sqrt{\frac{KT_1}{\phi_R(1-0.5\phi_R)^2 d_1^3 \mu}} \quad (12)$$

$$\sigma_{F|gear} = \frac{2KT_1 Y_{Fa} Y_{Sa}}{\phi_a m^3 z_1^2} \quad (13)$$

$$\sigma_{ca|axle} = \frac{\sqrt{M^2 + (\alpha T_1)^2}}{W} \quad (14)$$

$$L_{h|bearing} = \frac{10^6}{60n} \left(\frac{C}{P}\right)^\epsilon, P = f_p f_t (X F_R + Y F_A) \quad (15)$$

In the formula, $K=K_A K_a K_\beta K_V$, K_A is working condition coefficient, K_a is gear tooth load distribution coefficient, K_β is gear tooth direction load distribution coefficient, K_V is moving load coefficient, Y_{Fa} is tooth shape coefficient, Y_{Sa} is stress correction coefficient.

From the contact and bending strength check formula of the gear, it is concluded that the reducers don't have the disassembly economy criterion:

- (1) The gear tooth has cracks;
- (2) The gear tooth broken;
- (3) The points of the gear meshing faces corrosion damage up to 30%;
- (4) Any gear tooth thickness wears up to 10%.

Meet any of the four norms above, in accordance with the green disassembly standard, directly into P_{53} , P_{54} disassembly, remove harmful oil, and abandon the subsequent disassembly steps. Because the main purpose of this paper is to study the disassembly path, so reduce the probability of the bad gear conditions.

In summary, the green and economic disassembly of this paper uses the following criteria:

- (1) Find the shortest and best disassembly path, reduce the use of human and material resources, indirectly reduce energy consumption, and reduce pollutant emissions;
- (2) Toxic solid and liquid, even if the object to be disassembled has no disassembly value, disassemble it and remove the dangerous substance;

(3) If the value of re-repair or reuse is low, after the toxic waste removed, no further disassembly will be carried out.

2.4 Fuzzy disassembly time

In the process of disassembling the reducer, each part will have different disassembly time. To describe the uncertainty generated during the disassembly process, the triangular fuzzy number is used to indicate the fuzzy disassembly time of each part. The fuzzy time is expressed as: $P_{it}(t_{ia}, t_{ib}, t_{ic})$, in order to save the disassembly time, while avoiding damage to valuable parts, during the disassembly process, light parts and non-precious metal parts are reserved for smaller disassembly time, and more valuable parts are reserved more time. The disassembly time conversion and calculation formula are as follows:

$$t_i = \begin{cases} \left[\frac{t_{ia}+t_{ib}}{2}, \frac{200 \times m_i}{t_{ib}-t_{ia}} - \frac{t_{ia}}{t_{ib}-t_{ia}} < 1 \cup \text{material is cast iron} \right. \\ \left. t_{ib}, \text{otherwise} \right] & (16) \\ \left[\frac{t_{ib}+t_{ic}}{2}, \frac{200 \times m_i}{t_{ib}-t_{ia}} - \frac{t_{ia}}{t_{ib}-t_{ia}} > 1 \cap \text{material is not cast iron} \right] \end{cases}$$

$$(1) (t_{ia}, t_{ib}, t_{ic}) + (t_{ja}, t_{jb}, t_{jc}) = (t_{ia} + t_{ja}, t_{ib} + t_{jb}, t_{ic} + t_{jc})$$

$$(2) (t_{ia}, t_{ib}, t_{ic}) / (t_{ja}, t_{jb}, t_{jc}) = (t_{ia}/t_{ja}, t_{ib}/t_{jb}, t_{ic}/t_{jc})$$

$$(3) (t_{ia}, t_{ib}, t_{ic}) \times (\alpha_1, \alpha_2, \alpha_3) = (\alpha_1 t_{ia}, \alpha_2 t_{ib}, \alpha_3 t_{ic})$$

$$(4) (t_{ia}, t_{ib}, t_{ic}) \times (t_{ja}, t_{jb}, t_{jc}) = (t_{ia} t_{ja}, t_{ib} t_{jb}, t_{ic} t_{jc})$$

3. IMPROVED I-ACO FOR DLBP

Currently, the existing three-dimensional path planning algorithms mainly include: genetic algorithm, particle swarm algorithm, A* algorithm, ACO, etc. Genetic algorithm and particle swarm algorithm have complex coding, and the problem of solving discrete optimization problems is easy to fall into local optimum, and A* algorithm's calculation will increase dramatically as the number of dimensions increases. The ACO has the advantages of distributed computing and group intelligence. Therefore, the path planning of the disassembled object uses the improved Ant Colony Optimization.

Table 1. DLBP and TSP/DVRP corresponding relationship

DLBP	TSP/DVRP
Parts barycenter(3D)	City position(2D)
Parts	Client/City
Disassembly sequence	Travel sequence
Parts waiting disassembled	Unselected city/client
Disassembly cost	Travel cost
Alternative parts satisfy disassembly relationship and hasn't disassembled	Alternative city has not traveled yet
Optimize disassembly se-quences and reduce cost	The shortest route for travel or vehicle

Recently, the ACO is widely and deeply studied for the TSP/DVRP problem. The disassembly path planning of this paper has great similarities with the TSP and DVRP. The correspondence of DLBP and TSP/DVRP are as shown in Table 1. In this paper, I-ACO is used to solve the three-dimensional disassembly sequence and path planning.

3.1 FCM fuzzy clustering

The FCM (Fuzzy c-means) algorithm is proposed by Bezdek, the clustering algorithm for determining the attribution of data by affiliation degree. makes the object similarity between the same set to largest. It is an improvement of HCM. This paper uses the FCM algorithm to make n vector P_i is divided into c fuzzy groups, and the constraint value function J is minimized:

$$J(U, c_1, \dots, c_c) = \sum_{i=1}^c J_i = \sum_{i=1}^c \sum_{j=1}^n \mu_{ij}^m D_{ij}^2 \quad (17)$$

In the formula, the sum affiliation of μ is 1, c is the fuzzy clustering center, D_{ij} is the Euclidean distance between the parts P_i and P_j , and m is the control algorithm flexible parameter.

3.2 State transfer rules

The probability that the k th ant chooses next part j after part i disassembly [23] follows the formula:

$$P_{ij}(k) = \begin{cases} \frac{(\tau_{ij}(t))^\alpha \times (\eta_{ij}(t))^\beta}{\sum_{\mu \in Allowed_k} (\tau_{i\mu}(t))^\alpha \times (\eta_{i\mu}(t))^\beta}, & j \in Allowed_k; \\ 0, & j \notin Allowed_k. \end{cases} \quad (18)$$

$$Cost(i, j, k) = \xi_1 D(i, j, k) + \xi_2 T + 1000 M \xi_3 \quad (19)$$

In the formula, α denotes pheromone, β denotes relative weight parameter of the heuristic information, $\tau_{ij}(t)$ denotes the amount of information on the part (i, j) in the ant pathfinding process at time t , and $\eta_{ij}(t)$ is a heuristic function, which is reciprocal disassembly cost of the formula 19, $Allowed_k$ represents the set of parts that the k th ant can select, for example, after reaching point 54, selectable set are 55, 56.

3.3 Pheromone Update

When ants find food, they will emit pheromones [24-25]. Larger pheromone, greater attraction to ants. The three-dimensional point represented by each part updates the pheromone after each ant passes. The pheromone update consists of two sections: local update and global update. When the ant passes the part barycenter $P_n(x_n, y_n, z_n)$, the pheromone of the point P_n is reduced by local update to increase the ant select other unsearched points, avoided to fall into local optimum prematurely. The local pheromone update formula is as follows:

$$\tau_{ij}(t) = (1 - \gamma) \tau_{ij}(t) \quad (20)$$

Global update is to increase the pheromone value of the shortest path node in the set when the ant completes path search. The global pheromone update formula is as follows:

$$\tau_{ij}(t) = (1 - \delta) \tau_{ij}(t) + \delta \Delta \tau_{ij} \quad (21)$$

δ represents the degree volatilization of the pheromone, and the value is (0,1). The equation of $\Delta \tau_{ij}(t)$ is as follows:

$$\Delta \tau_{ij}(t) = \begin{cases} \frac{Q}{K \times L_k} \times \frac{D^{k-D_{ij}}}{P^k \times D^k}, & (i, j) \in \text{Global optimal path} \\ 0, & (i, j) \notin \text{Global optimal path} \end{cases} \quad (22)$$

In formula 22, $L_k = \sum_1^k D^k$, D^k is the length of the k th road, D_{ij} is the distance between parts i, j , and P^k is the part number. Which can be obtained from the above formula, the pheromone increment $\Delta \tau_{ij}(t)$ is inversely proportional to the distance $L(i)$, hence, the shortest path is more attractive to the ant colony. Due to global optimum when pheromone update, the information of some edges may be much higher than other edges. The ant repeatedly selects the edge, stops exploring the search space, and falls into the local optimal solution too early, but by limiting the maximum value of the pheromone trajectory τ_{min}, τ_{max} , the oversize difference of the pheromone trajectory in the algorithm operation can be avoided. The pheromone trajectory maximum value [26] is set as follows:

$$\tau_{min} = \frac{Q}{\sum_1^i 2D_{1i}}, (1 < i \leq 84); \quad (23)$$

$$\tau_{max} = \frac{Q}{\sum_1^i D_{1i}}, (1 < i \leq 84); \quad (24)$$

D_{1i} indicates the distance between the i th part and the first part.

3.4 Dynamic candidate table $Allowed_k$

In order to improve the search efficiency of I-ACO, the number of parts selected each time should be limited to the appropriate candidate list. This method is called candidate set strategies, and the search is traversed according to the candidate table $Allowed_k$. In this paper, the dynamic candidate table strategy is adopted. $Allowed_k$ is continuously updated in the search process. The advantage of ant algorithm is derived from the use of adaptive memory ie pheromone trajectory. Therefore, using dynamic candidate list strategy can further improve the quality of the solution and calculation operation time. Dynamic candidate table $Allowed_k$ update rules are as follows:

- (1) When running the I-ACO to start searching for the disassembly path, $Allowed_k$ are P_1, P_9, P_{10} three parts;
- (2) The upper side connection relationship in the R-AOG diagram has been removed, and P_i is added to the $Allowed_k$;
- (3) After the part P_i is disassembled, the corresponding disassembly constraint and node in the R-AOG will be deleted;
- (4) The parts in $Allowed_k$ must be completely disassembled before update the candidate table. For example, P_{65}, P_{76}, P_{83} must be disassembled before update P_{84} to $Allowed_k$.

3.5 2-Opt

2-Opt is a classical heuristic algorithm proposed by Croes in 1958 [27-29]. The main idea is to exchange the paths of two adjacent positions to obtain the optimal solution and avoid the algorithm falling into local optimum.

Table 2 and Figure 4 is an example of a 2-Opt exchange algorithm. Component PB(66-70) and PB(71-75), there is no constraint relationship between R-AOG. In Figure 4, B1 is selected two better paths, the disassembly sequence before the exchange is: 51-52-53-54-56-55-B(66-70)-B(71-75)-76. After the exchange, the disassembly sequence of B2 is: 51-52 -53-54-56-55-B(71-75)-B(66-70)-76.

Table 2. Parts 51-76 constraint information

Parts No.	51	52	53	54	56	55	B(66-70)	B(71-75)	76
Predecessors	49 OR 50	51	52	53	52	52	55 AND 56	55 AND 56	66-75(AND)
PN	1	1	1	1	1	1	2	2	10

Table 3. Gear reducer disassembly parts information

Number	Task and Part Name NAME	Disassembly Parameter					Location		
		fuzzy t	Cost	M/kg	Tool	After	X	Y	Z
1	Cap nut	(2,3,4)	0.0029	0.006	T _H	START	-110	60.6	-166
2	Cross recessed screw 1	(3,5,7)	0.0033	0.002	T _S	1	-195	47.5	-211
3	Cross recessed screw 2	(3,5,7)	0.0033	0.002	T _S	1	-110	47.5	-211
4	Cross recessed screw 3	(3,5,7)	0.0033	0.002	T _S	1	-25.5	47.5	-211
5	Cross recessed screw 4	(3,5,7)	0.0033	0.002	T _S	1	-25.5	47.5	-121
6	Cross recessed screw 5	(3,5,7)	0.0033	0.002	T _S	1	-110	47.5	-121
7	Cross recessed screw 6	(3,5,7)	0.0033	0.002	T _S	1	-195	47.5	-121
8	Cover	(14,16,18)	0.0027	0.082	T _H	2~7	-110	49.9	-166
9	High speed axis key	(13,15,17)	0.0053	0.028	T _P	START	-312	-76.3	-232
10	Output axis key	(13,15,17)	0.0053	0.028	T _P	START	126	-83.4	-212
11	A Hex Bolts 1	(6,8,10)	0.0035	0.015	T _{W1}	8	-268	-44.3	-232
12	A Hex Bolts 2	(6,8,10)	0.0035	0.015	T _{W1}	8	-268	-64.8	-196
13	A Hex Bolts 3	(6,8,10)	0.0035	0.015	T _{W1}	8	-268	-106	-196
14	A Hex Bolts 4	(6,8,10)	0.0035	0.015	T _{W1}	8	-268	-126	-232
15	A Hex Bolts 5	(6,8,10)	0.0035	0.015	T _{W1}	8	-268	-106	-268
16	A Hex Bolts 6	(6,8,10)	0.0035	0.015	T _{W1}	8	-268	-64.8	-268
17	A Bearing cap	(1,2,3)	0.0027	0.075	T _H	11~16	-267	-85.3	-232
18	B Hex Bolts 1	(6,8,10)	0.0035	0.015	T _{W1}	8	-268	-40.3	-101
19	B Hex Bolts 2	(6,8,10)	0.0035	0.015	T _{W1}	8	-268	-62.2	-61
20	B Hex Bolts 3	(6,8,10)	0.0035	0.015	T _{W1}	8	-268	-107	-61
21	B Hex Bolts 4	(6,8,10)	0.0035	0.015	T _{W1}	8	-268	-130	-101
22	B Hex Bolts 5	(6,8,10)	0.0035	0.015	T _{W1}	8	-268	-108	-139
23	B Hex Bolts 6	(6,8,10)	0.0035	0.015	T _{W1}	8	-268	-63.3	-139
24	B Bearing cap	(1,2,3)	0.0027	0.100	T _H	18~23	-267	-85.3	-100
25	C Hex Bolts 1	(6,8,10)	0.0035	0.015	T _{W1}	8	47.2	-30.3	-232
26	C Hex Bolts 2	(6,8,10)	0.0035	0.015	T _{W1}	8	47.2	-57.8	-280
27	C Hex Bolts 3	(6,8,10)	0.0035	0.015	T _{W1}	8	47.2	-113	-280
28	C Hex Bolts 4	(6,8,10)	0.0035	0.015	T _{W1}	8	47.2	-140	-232
29	C Hex Bolts 5	(6,8,10)	0.0035	0.015	T _{W1}	8	47.2	-113	-184
30	C Hex Bolts 6	(6,8,10)	0.0035	0.015	T _{W1}	8	47.2	-57.8	-184
31	C Bearing cap	(1,2,3)	0.0027	0.959	T _H	25~30	45.7	-85.3	-232
32	D Hex Bolts 1	(6,8,10)	0.0035	0.015	T _{W1}	8	47.2	-39.3	-100
33	D Hex Bolts 2	(6,8,10)	0.0035	0.015	T _{W1}	8	47.2	-62.3	-140
34	D Hex Bolts 3	(6,8,10)	0.0035	0.015	T _{W1}	8	47.2	-108	-140
35	D Hex Bolts 4	(6,8,10)	0.0035	0.015	T _{W1}	8	47.2	-131	-100
36	D Hex Bolts 5	(6,8,10)	0.0035	0.015	T _{W1}	8	47.2	-108	-60
37	D Hex Bolts 6	(6,8,10)	0.0035	0.015	T _{W1}	8	47.2	-62.3	-60
38	D Bearing cap	(1,2,3)	0.0027	0.100	T _H	32~37	45.8	-85.3	-100
39	E Hex Bolts 1	(13,16,19)	0.0055	0.115	T _{W2}	8	-239	-85.9	-35
40	E Hex Bolts 2	(13,16,19)	0.0055	0.115	T _{W2}	8	-239	-85.9	-169
41	E Hex Bolts 3	(13,16,19)	0.0055	0.115	T _{W2}	8	-239	-85.9	-296
42	E Hex Bolts 4	(8,10,12)	0.0043	0.072	T _{W2}	8	-175	-86.6	-376
43	E Hex Bolts 5	(8,10,12)	0.0043	0.072	T _{W2}	8	-45.5	-86.6	-376
44	E Hex Bolts 6	(13,16,19)	0.0055	0.115	T _{W2}	8	18.5	-85.9	-302
45	E Hex Bolts 7	(13,16,19)	0.0055	0.115	T _{W2}	8	18.5	-85.9	-160
46	E Hex Bolts 8	(13,16,19)	0.0055	0.115	T _{W2}	8	18.5	-85.9	-35
47	E Hex Bolts 9	(8,10,12)	0.0043	0.072	T _{W2}	8	-45.5	-86.6	43.5
48	E Hex Bolts 10	(8,10,12)	0.0043	0.072	T _{W2}	8	-175	-86.6	43.5
49	Tapered pin 1	(2,3,4)	0.0029	0.006	T _{W2}	39~48	-205	-85.2	-376
50	Tapered pin 2	(2,3,4)	0.0029	0.006	T _{W2}	49	-15.5	-85.1	43.5
51	Up-Down Bolt	(1,3,5)	0.0031	0.054	T _{W2}	50	-205	-56.6	43.5
52	Upper reducer box	(12,15,18)	0.0053	2.700	T _H	51	-111	-27.9	-166
53	Oil Cursor	(1,2,3)	0.0027	0.008	T _H	52	-176	-141	-372
54	Oil Drain Bolt (include drain oil)	(37,40,43)	0.103	0.004	T _{W2}	END	-110	-211	32.4
55	Stud 1	(8,10,12)	0.0043	0.067	T _{W2}	START	-113	-68.7	-302
56	Stud 2	(8,10,12)	0.0043	0.067	T _{W2}	START	-113	-68.7	-162
57	Bearing up cover	(2,3,4)	0.0029	0.134	T _H	56	-113	-59.2	-232
58	Bearing spacer	(2,3,4)	0.0029	0.015	T _C	57	-242	-85.3	-232

59	Tapered Roller Bearing 30206(R)	(14,16,18)	0.0061	0.213	T _C	58	-224	-85.3	-232
60	Bearing spacer	(2,3,4)	0.0029	0.051	T _C	59	-209	-85.3	-232
61	High Speed Shaft Gear	(10,13,16)	0.0049	0.073	T _{HA}	60	-179	-85.7	-232
62	High Speed Shaft Key	(13,15,17)	0.0053	0.024	T _P	61	-178	-67.8	-232
63	Bearing spacer	(2,3,4)	0.0029	0.527	T _C	55	-127	-85.3	-232
64	Tapered Roller Bearing 30206(L)	(14,16,18)	0.0061	0.213	T _C	55	-129	-85.3	-232
65	High Speed Shaft	(1,3,5)	0.0029	0.138	T _H	58~64	-202	-85.3	-232
66	Bearing spacer	(2,3,4)	0.0029	0.016	T _C	55	-241	-85.3	-100
67	Tapered Roller Bearing30306(R)	(14,16,18)	0.0061	0.352	T _C	66	-222	-85.3	-100
68	Bearing spacer	(2,3,4)	0.0029	0.072	T _C	67	-206	-85.3	-100
69	Intermediate Shaft Big Gear	(10,13,16)	0.0049	0.536	T _{HA}	68	-179	-85.3	-100
70	Intermediate Shaft Key 1	(13,15,17)	0.0053	0.021	T _P	69	-178	-81.3	-117
71	Bearing spacer	(2,3,4)	0.0029	0.016	T _C	55	20.2	-85.3	-100
72	Tapered Roller Bearing 30306(L)	(14,16,18)	0.0061	0.352	T _C	71	5.48	-85.3	-100
73	Bearing spacer	(2,3,4)	0.0029	0.045	T _C	72	-8.72	-85.3	-100
74	Intermediate Shaft Small Gear	(10,13,16)	0.0049	0.094	T _{HA}	73	-44.5	-85.4	-100
75	Intermediate Shaft Key 2	(13,15,17)	0.0053	0.033	T _P	74	-45.5	-81.4	-116
76	Intermediate Shaft	(1,3,5)	0.0029	2.130	T _H	66~75	-110	-85.3	-100
77	Tapered Roller Bearing 30210(R)	(15,17,19)	0.0061	0.501	T _C	55	-100	-85.3	-232
78	Sleeve	(2,3,4)	0.0029	0.125	T _C	77	24.6	-85.3	-232
79	Tapered Roller Bearing 30210(L)	(15,17,19)	0.0061	0.501	T _C	55	5.1	-85.3	-232
80	Sleeve	(2,3,4)	0.0029	0.066	T _C	79	-10.5	-85.3	-232
81	Output Shaft Gear	(10,13,16)	0.0049	0.965	T _{HA}	80	-44.5	-85.3	-232
82	Output Shaft Key	(13,15,17)	0.0053	0.058	T _P	81	-44.5	-82.7	-205
83	Output Shaft	(1,3,5)	0.0029	3.720	T _H	77~82	3.21	-85.3	-232
84	Lower reducer box	(12,15,18)	0.0053	5.000	T _H	END	-111	-175	-170

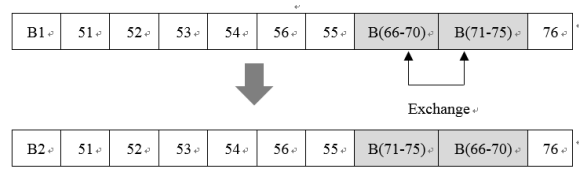


Figure 4. 2-Opt optimization

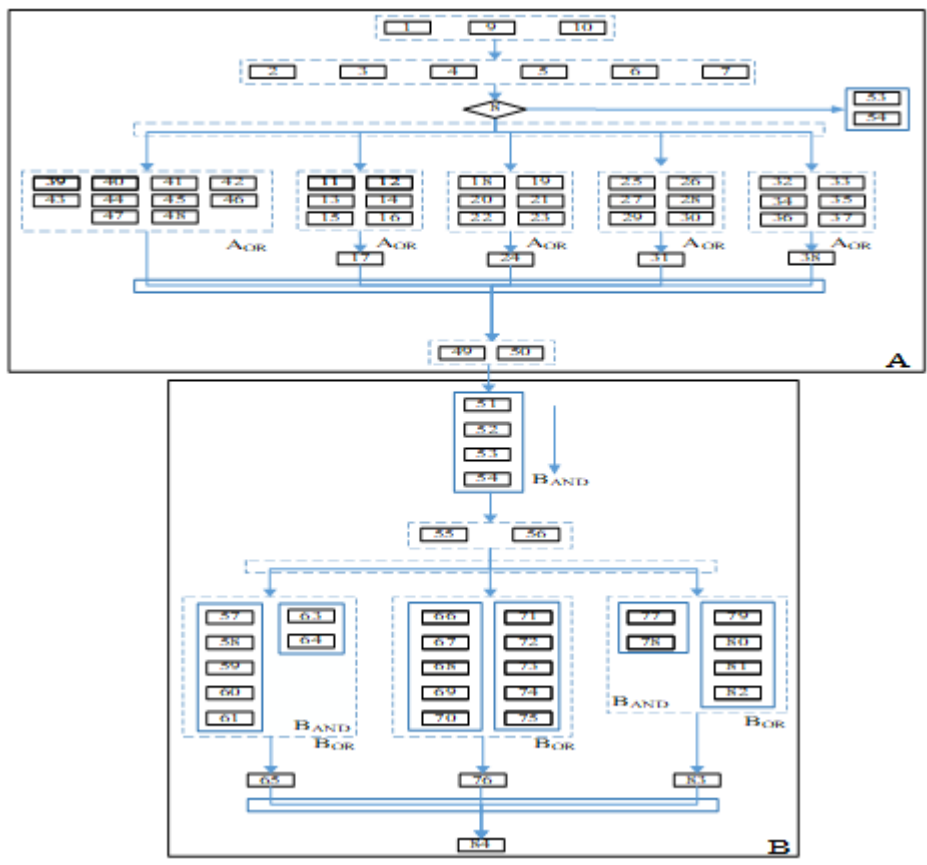


Figure 5. Reducer R-AOG

3.5 Algorithm steps

- Step1 Initialize parameters $\alpha, \beta, \gamma, Q, M, n, t, NC_max$;
- Step 2 Generates adjacency matrix $D(i, j)$ stores the distance;
- Step3 Initializes the dynamic update candidate table $A_ollwedk$, transition probability P_{ij} ;
- Step4 Construction path;
- Step5 Applies the local update $t_{ij}(t)$;
- Step 6 Judge whether a circulation ends;
- Step7 Records the parameters of this generation;
- Step8 Performs 2-Opt optimization;
- Step 9 Performs a global update $t_{ij}(t)$;
- Step 10 Judge whether the circulation reaches the maximum number of iterations NC_max ;
- Step11 Outputs the parameters such as the optimal disassembly sequence and plots;
- Step12 I-ACO ends.

4. EXPERIMENTAL AND DISSCUSSIONS

Since the research on disassembly path of WMEP using three dimensional coordinates has not been found yet, in order to verify the efficiency and correctness of the proposed I-ACO, the I-ACO is validated by the current research on TSP/DVRP, and the corresponding data set is selected to compare the I-ACO with ACO, E-ACO [30-31]. Because the path planning is two-dimensional, the distribution between nodes has no constraint relationship, so the above FCM algorithm is adjusted to K-means, the error means square formula [32] is as follows:

$$J_c = \sum_{i=1}^k \sum_{P \in X_i} \| P - A_i \|^2 \quad (25)$$

X_i is the clustering center, P is the data contained in the i clustering center, A_i is the mean of the i clustering center data, and the traditional K-means clustering, the wrong K value will have an important influence on the algorithm. In the algorithm, the distance cost function F_{cost} [33] is used to determine the K value. The formula is as follows:

$$F_{cost} = \sum_{i=1}^k |A_i - \bar{A}| + \sum_{i=1}^k |P - A_i| \quad (26)$$

\bar{A} represents the mean of all data, and when F_{cost} reaches the minimum, the best cluster is obtained. The I-ACO running on MATLAB R2016a, the configuration is Core (TM) i5-8250U CPU 1.6GHz, 8GB RAM, 64-bit Windows10, Running 30 times per data set, recording the optimal solution and mean after running the algorithm. ACO, E-ACO, I-ACO is compared, the specific data is in Table 4. The optimal solution obtained by each algorithm is bolded. The I-ACO obtains 18 optimal solutions and 22 mean optimal solutions. When the number of nodes in the data set is less than 100, the I-ACO obtains the optimal solution and the optimal mean of 12, accounting for 85.7%. The number of disassembled parts in this paper is 84, which proves that I-ACO designed to the disassembly sequence can be effective.

Finally, the algorithm is applied to the reducer disassembly path planning solution. Since the disassembly line solution is the NP-Complete problem, the number of disassembly tools, remove hazardous parts, the shortest disassembly distance and minimum energy consumption index as the solution target. Due to the large number of parts, the disassembly path

is divided into the external disassembly path and the internal disassembly path of the reducer. After the I-ACO is run, the optimal distance of the external disassembly path is calculated to be 4365.20mm, the disassembly tool is changed 6 times, and the energy consumption index is 350.699, the toxic liquid is removed once. The specific path is shown in Figure 7. The optimal distance of the internal disassembly path is 1493.171mm, the disassembly tool is changed 10 times, and the energy consumption index is 518.872. The results meet the requirements of I-ACO to increase the weight of disassembly high-value components. The specific path is shown in Figure 8, and the specific disassembly sequence in the outside of the box and in the box is shown in Table 5. Figure 6 is a view showing incomplete disassembly of the speed reducer when the gear unit is inspected after the green and economic disassembly criterion is followed. The specific path is shown in Figure 6.

Table 4. ACO, E-ACO, I-ACO result comparison

Name	ACO		E-ACO		I-ACO		Nodes
	Best	Average	Best	Average	Best	Average	
c50	631.30	681.86	607.21	647.21	553.88	593.45	52
c75	1009.36	1042.39	924.71	1045.44	806.47	836.56	77
c100	973.26	1066.16	973.40	1044.96	984.08	1030.02	102
c100b	944.23	1023.60	869.22	950.17	598.73	657.81	102
c120	1416.45	1525.15	1108.15	1197.68	701.66	774.85	122
c150	1345.73	1455.50	1378.63	1472.40	1240.51	1348.01	145
c199	1771.04	1844.82	1561.12	1836.86	1789.53	1822.21	168
f71	311.18	358.69	259.71	297.08	245.53	293.82	73
fl35	-	-	-	-	964.92	1174.80	136
tai75a	1843.08	1945.20	1690.91	1983.00	1728.61	1790.06	83
tai75b	1535.43	1704.06	1509.56	1647.78	1342.20	1459.10	84
tai75c	1574.98	1653.58	1329.42	1470.60	1388.10	1456.60	84
tai75d	1472.35	1529.00	1409.14	1661.73	1402.80	1527.80	84
tail00a	2375.92	2428.38	2281.70	2550.64	2389.70	2509.40	109
tail00b	2283.97	2347.90	2255.83	2500.72	2245.70	2425.20	111
tail00c	1562.30	1655.91	1442.45	1743.07	1766.00	1862.80	112
tail00d	2008.13	2060.72	1581.36	1843.82	2015.50	2088.50	108
tail50a	3644.78	3840.18	3307.63	3684.03	3594.70	3681.10	162
tail50b	3166.88	3327.47	3128.00	3439.38	3082.50	3340.02	163
tail50c	2811.48	3016.14	2583.36	2729.15	3057.20	3173.10	166
tail50d	3058.87	3203.75	2808.99	3186.08	2744.60	2928.40	164
kelly06	-	-	-	-	15373.00	15422.00	283
kelly07	-	-	-	-	17268.00	18095.00	363
kelly08	-	-	-	-	19005.00	20323.00	442
kelly09	868.62	936.35	830.98	906.71	730.57	745.44	256
kelly10	1181.00	1243.90	1072.50	1244.70	983.18	1039.60	325
kelly11	1415.40	1618.30	1311.10	1523.60	1282.90	1342.70	402
kelly12	1722.80	2047.50	1755.80	2068.90	1660.00	1736.90	485
kelly13	1108.80	1232.20	1096.00	1188.90	898.19	970.02	256
kelly14	1526.50	1649.10	1363.10	1548.20	1235.20	1293.00	323
kelly15	1784.90	1960.00	1781.40	1861.00	1631.90	1659.20	399
kelly16	1476.40	1641.24	1429.39	1598.04	1546.50	1703.10	483
SUM	1	3	8	2	18	22	

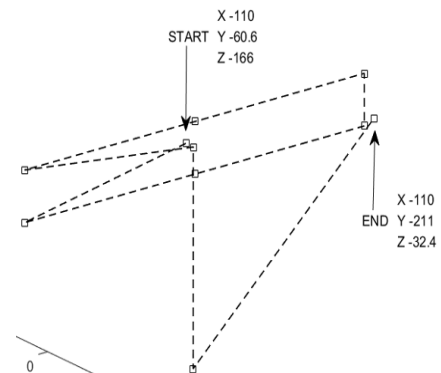


Figure 6. Incompletely disassembled

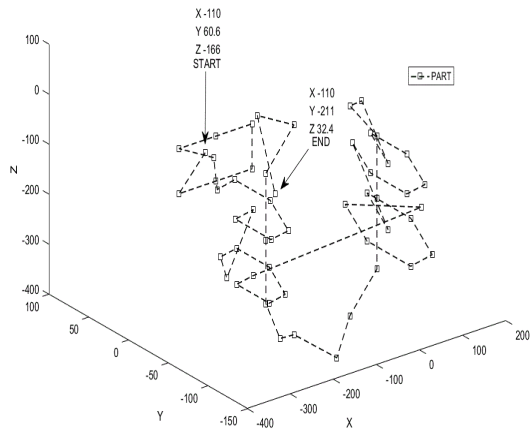


Figure 7. External reducer parts disassembly path

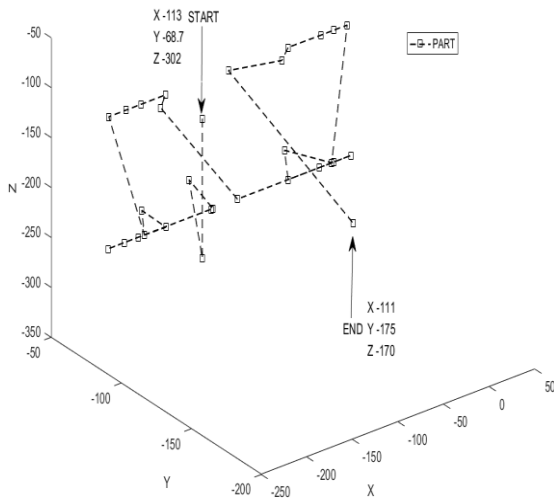


Figure 8. Internal reducer parts disassembly path

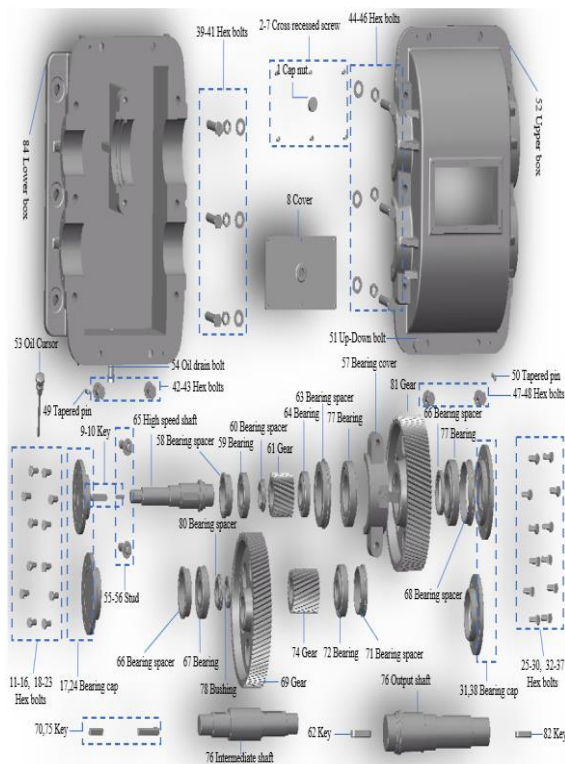


Figure 9. Gear reducer component parts

Table 5. Reducer optimal disassembly sequence and disassembly parameters

Section	Task	I-ACO				
		Disassembly Best Route	Length	f_1	f_2	f_3
Out-Reducer	54	1-2-3-4-5-6-7-8-18-19-20-21-22-23-24-9-11-12-13-14-15-16-17-10-25-26-27-28-29-30-31-32-33-34-35-36-37-38-50-47-46-45-44-43-53-42-49-41-40-39-48-51-52	4365.208	6	350.699	1
		56-55-57-63-64-58-59-60-61-62-65-66-67-68-69-70-77-78-79-80-81-82-83-71-72-73-74-75-76-84				
In-Reducer	30	67-68-69-70-77-78-79-80-81-82-83-71-72-73-74-75-76-84	1493.171	10	518.872	0

5. CONCLUSIONS AND FUTURE WORK

Disassembly Line research is of great significance to the product life cycle management. In this paper, the reducer disassembly is taken as example. For the problem that the disassembly line is not currently studied in the three-dimensional position, green and economic angle of the disassembly object, the following research is made:

(1) Improve the traditional AOG directed graph, and use the virtual and solid rectangle to represent the directional constraint of the component. When describing the large-scale disassembly object, the R-AOG graph has the advantages of easy writing and clearer component constraints.

(2) Using the FCM, 2-Opt, dynamic candidate table Allowed_k and other methods improve ACO to I-ACO, and select the dataset such as kelly, compare with other algorithms to verify the effectiveness of the algorithm;

(3) Using 3D drawing software, the physical reducer is mapped, and the 3D coordinates of the reducer are obtained. By strength check formula of the main components such as shaft, bearing and gear, decided to use the maintenance status of the gear as the economic criteria for disassembly. Use fuzzy correction time to ensure sufficient disassembly time of high-value parts. At the same time, because WMEP contain environment-ally harmful substances, in order to adhere the green production guidelines, this paper proposes that when determining the disassembly object has no corresponding economic value, exclude toxic solid liquid and give up complete disassembly;

(4) Using the I-ACO to obtain the disassembly line path. Since the disassembly line is the NP-Complete problem, this paper obtains the corresponding disassembly line with the minimum optimization of the number disassembly tools, the minimum disassembly distance, and the lowest energy consumption index. If this path is programmed into the vehicle reducer using maintenance manual, it will greatly reduce the maintenance threshold of the reducer and beneficial to build automated disassembly lines, which is of great significance for reducing the use cost and indirectly reducing the resource consumption.

The next research work: (i). study the robotic automatic disassembly, because the robot walking path does not allow diagonal walking, can only walk vertically and horizontally, and then study the use of Manhattan distance $D_{ij}=|x_j-x_i|+|y_j-$

$y_i + |z_j - z_i|$ instead of Euclidean distance; (ii). I-ACO achieves 85.7% optimal value in 100 data sets, but still there is room for improvement, and will continue to improve research.

ACKNOWLEDGEMENTS

This work was financially supported by Chinese University Students Innovation Fund Project (201411585002Y).

REFERENCES

- [1] Ministry of Commerce of the People's Republic of China Department of Circulation Industry Development. Development report of Recycled Resources Recycling Industry of China (2016). *Recycling Research* 9(6): 15-21.
- [2] Zhang ZQ, Wang KP, Li LK. (2018). Multi-objective optimization for U-shaped disassembly line balancing problem with stochastic operation times. *Computer Integrated Manufacturing Systems* 24(1): 89-100.
- [3] Zhang L, Liu ZF, Yang M. (2011). Disassembly sequence planning based on interpretative structural model. *Journal of Computer-Aided Design & Computer Graphics* 23(4): 667-675.
- [4] Song XW, Pan XX. (2011). Electromechanical product disassembly sequence planning based on partial destruction mode. *Computer Integrated Manufacturing Systems* 18(5): 927-931.
- [5] Kalaycılar EG, Azizoglu M, Yeralan S. (2016). A disassembly line balancing problem with fixed number of workstations. *European Journal of Operational Research* 249(2). <https://doi.org/10.1016/j.ejor.2015.09.004>
- [6] Kalayci CB, Hancilar A, Gupta AM. (2014). Multi-objective fuzzy disassembly line balancing using a hybrid discrete artificial bee colony algorithm. *Journal of Manufacturing Systems* 37. <https://doi.org/10.1016/j.jmsy.2014.11.015>
- [7] Mete S, Çil ZA, Ağpak K, Özceylan E, Dolgui A. (2016). A solution approach based on beam search algorithm for disassembly line balancing problem. *Journal of Manufacturing Systems* 41. <https://doi.org/10.1016/j.jmsy.2016.09.002>
- [8] Ren YP, Zhang CY, Zhao F, Tian GD, Lin WW, Meng LL, Li HL. (2018). Disassembly line balancing problem using interdependent weights-based multi-criteria decision making and 2-Optimal algorithm. *Journal of Cleaner Production* 174. <https://doi.org/10.1016/j.jmsy.2016.09.002>
- [9] Tian G, Zhou MC, Chu JA. (2013). Chance constrained programming approach to determine the optimal disassembly sequence. *IEEE Transactions on Automation Science & Engineering* 10(4): 1004-1013. <http://doi.org/10.1109/TASE.2013.2249663>
- [10] Ren YP, Tian GD, Zhao F, Yu DY, Zhang CY. (2017). Selective cooperative disassembly planning based on multi-objective discrete artificial bee colony algorithm. *Engineering Applications of Artificial Intelligence* 64. <https://doi.org/10.1016/j.engappai.2017.06.025>
- [11] Zhang ZQ, Wang KP, Zhu LX, Wang Y. (2017). A Pareto improved artificial fish swarm algorithm for solving a multi-objective fuzzy disassembly line balancing problem. *Expert Systems with Applications* 86. <https://doi.org/10.1016/j.eswa.2017.05.053>
- [12] Liu JY, Zhou ZD, Duc Truong Pham, Xu WJ, Yan JW, Liu AM, Ji CQ, Liu Q. (2018). An improved multi-objective discrete bees algorithm for robotic disassembly line balancing problem in remanufacturing. *The International Journal of Advanced Manufacturing Technology* 97(9-12). <https://doi.org/10.1007/s00170-018-2183-7>
- [13] Mohand LB, Olga B, Alexandre D. (2014). Lagrangian relaxation for stochastic disassembly line balancing problem. *Procedia CIRP* 17. <https://doi.org/10.1016/j.procir.2014.02.049>
- [14] Süleyman M, Zeynel AÇ, Eren Ö, Kürşad A. (2016). Resource constrained disassembly line balancing problem. *IFAC Papers on Line* 49(12). <https://doi.org/10.1016/j.procir.2014.02.049>
- [15] Robert JR, Olga BS, Jack H. (2015). Disassembly line balancing under high variety of end of life states using a joint precedence graph approach. *Journal of Manufacturing Systems* 37. <https://doi.org/10.1016/j.jmsy.2014.11.002>
- [16] Naveen K, Doshi JB, Vijayan PK. (2011). Investigations on the phenomenon of hysteresis in single-phase natural circulation loops. *Smirt*. <https://doi.org/10.18280/mmep.050305>
- [17] Turan P, Aşkın G, Eren Ö, Arif H. (2013). Mixed model disassembly line balancing problem with fuzzy goals. *International Journal of Production Research* 51(20). <https://doi.org/10.1080/00207543.2013.795251>
- [18] Agrawal S, Tiwari MK. (2006). A collaborative ant colony optimization to stochastic mixed-model U-shaped disassembly line balancing and sequencing problem. *International Journal of Production Research* 46(6). <https://doi.org/10.1080/00207540600943985>
- [19] Mohand LB, Olga B, Alexandre D. (2013). Chance constrained programming model for stochastic profit-oriented disassembly line balancing in the presence of hazardous parts. *Springer Berlin Heidelberg*. https://doi.org/10.1007/978-3-642-41266-0_13
- [20] Ali K, Ihsan S, Erdal E. (2009). Two exact formulations for disassembly line balancing problems with task precedence diagram construction using an AND/OR graph. *IIE Transactions* 41(10). <https://doi.org/10.1080/07408170802510390>
- [21] Tevhid F, Altekin, Levent K, Nur EO. (2007). Profit-oriented disassembly line balancing. *International Journal of Production Research* 46(10). <https://doi.org/10.1080/00207540601137207>
- [22] Yigit K, Yucel O. (2018). Integrated framework of disassembly line balancing with Green and business objectives using a mixed MCDM. *Journal of Cleaner Production* 191. <https://doi.org/10.1016/j.jclepro.2018.04.189>
- [23] Yu B, Yang ZZ, Yao BZ. (2008). An improved ant colony optimization for vehicle routing problem. *European Journal of Operational Research* 196(1). <https://doi.org/10.1016/j.ejor.2008.02.028>
- [24] Dorigo M, Gambardella LM. (1997). Ant colony system: A cooperative learning approach to the traveling salesman problem. *IEEE Trans. on Evolutionary Computation* 1(1):53-66.

- [25] Dorigo M, Maniezzo V. (1991). Positive Feedback as a Search Strategy. Technical Report.
- [26] Yang ZZ, Yu B, Cheng CT. (2007). A parallel ant colony algorithm for bus network optimization. *Computer Aided Civil and Infrastructure Engineering* 22(1). <https://doi.org/10.1111/j.1467-8667.2006.00469.x>
- [27] Croes GA. (1958). A method for solving traveling salesman problems. *Operations Research* 6(6). <https://doi.org/10.1287/opre.6.6.791>
- [28] McGovern SM, Gupta SM. (2005). A balancing method and genetic algorithm for disassembly line balancing. *European Journal of Operational Research* 179(3). <https://doi.org/10.1016/j.ejor.2005.03.055>
- [29] Ravi K, Diptesh G. (2013). Tabu search for the single row facility layout problem using exhaustive 2-opt and insertion neighborhoods. *European Journal of Operational Research* 224(1). <https://doi.org/10.1016/j.ejor.2012.07.037>
- [30] Montemanni R, Gambardella LM, Rizzoli AE. (2002). A new algorithm for a dynamic vehicle routing problem based on ant colony system. *Second International Workshop on Freight Transportation & Logistics*, 27-30.
- [31] Xu HT, Pu P, Duan F, Gabriella Bretti. (2018). Dynamic vehicle routing problems with enhanced ant colony optimization. *Discrete Dynamics in Nature and Society* 2018. <https://doi.org/10.1155/2018/1295485>
- [32] Gao SC, Wang YR, Cheng JJ, Inazumi Y, Tang Z. (2016). Ant colony optimization with clustering for solving the dynamic location routing problem. *Applied Mathematics and Computation* 285. <https://doi.org/10.1016/j.amc.2016.03.035>
- [33] Su MC, Chou CH. (2001). A modified version of the K-means algorithm with a distance based on cluster symmetry. *IEEE Computer Society*, <https://doi.org/2001.10.1109/34.927>.